INSTITUTE OF PHYSICS PUBLISHING PHYSICS IN MEDICINE AND BIOLOGY

Phys. Med. Biol. **49** (2004) 557–569 PII: S0031-9155(04)69327-4

Three-dimensional seed reconstruction for prostate brachytherapy using Hough trajectories

Steve T Lam[1], **Paul S Cho**[1,2], **Robert J Marks II**[3] **and Sreeram Narayanan**[1]

[1] Department of Electrical Engineering, University of Washington, Seattle, WA 98195-2500, USA
[2] Department of Radiation Oncology, School of Medicine, University of Washington, Seattle, WA 98195-6043, USA
[3] Department of Engineering, Baylor University, Waco, TX 76798-7356, USA

E-mail: psncho@u.washington.edu

Received 18 September 2003, in final form 15 December 2003
Published 27 January 2004
Online at stacks.iop.org/PMB/49/557 (DOI: 10.1088/0031-9155/49/4/007)

Abstract

In order to perform intra-operative or post-implant dosimetry in prostate brachytherapy, the 3D coordinates of the implanted radioactive seeds must be determined. Film or fluoroscopy based seed reconstruction techniques use back projection of x-ray data obtained at two or three x-ray positions. These methods, however, do not perform well when some of the seed images are undetected. To overcome this problem we have developed an alternate technique for 3D seed localization using the principle of Hough transform. The Hough method utilizes the fact that, for each seed coordinate in three dimensions, there exists a unique trajectory in Hough feature space. In this paper we present the Hough transform parametric equations to describe the path of the seed projections from one view to the next and a method to reconstruct the 3D seed coordinates. The results of simulation and phantom studies indicate that the Hough trajectory method can accurately determine the 3D seed positions even from an incomplete dataset.

1. Introduction

Brachytherapy seed reconstruction techniques from projection radiographs were actively developed in the early 1980s when interstitial implants were becoming widespread. Amols and Rosen (1981) introduced a three-film technique (a set of two stereo and one AP films) that eliminated the ambiguity in 3D seed locations arising from the use of only two films. Likewise, Rosenthal and Nath (1983) proposed a method that used three films. Their method differed from that of Amols and Rosen in that the projections were obtained with gantry rotation rather than from a stereo-shift. A similar method was developed independently by Biggs and Kelley (1983). Altschuler *et al* (1983) utilized three non-coplanar projections to

further reduce the ambiguity in seed matching. Their technique also addressed the problem of patient motion by using a fiducial marker. Siddon and Chin (1985) devised a two-film technique that employed the seed endpoints rather than the centroids to minimize the problem of ambiguous seed identification. More recently, prompted by the need for intra-operative dosimetry of prostate brachytherapy (Nag *et al* 2000), there has been a renewed interest in seed reconstruction. Tubic *et al* (2001) developed a method based on simulated annealing. A fast reconstruction method capable of handling up to four films was introduced by Narayanan *et al* (2002). Todor *et al* (2002) designed an algorithm using a set of heuristic rules towards improved accuracy.

The major limitation of current methods is the requirement that all the seeds must be identified in each of the 2D projection data in order to reconstruct 100% of the implanted seeds. However, with the large number of seeds used in prostate implants, it is often the case that the seed images are heavily clustered. Superimposed seeds are difficult or impossible to detect, thereby resulting in incomplete seed localization. We propose a new approach to 3D seed reconstruction using the concept of the Hough transform. Compared to the presently used back projection methods, the Hough trajectory method works in forward projection. Applying the Hough transform parametric equations to describe the path of the seeds from projection to projection, it is possible to uniquely identify the 3D seed positions even when some of the seeds are missing in the 2D data. The Hough trajectory method also has the ability to incorporate additional views without incurring major computing cost. The feasibility of the Hough technique was demonstrated in our previous work (Lam *et al* 2002). In the present paper, we report on further refinement of the technique and performance evaluation. Throughout the paper the term 'view' is used to denote the 2D seed data formed by conical x-ray projection.

2. Methods

2.1. Coordinate system

For convenience, a rotating coordinate system is used (figure 1). The reference coordinate system, in which the 3D seed centroid positions are ultimately determined, is given by (X, Y, Z). The x-ray source, located at Z, rotates about the Y-axis through angle θ. The seed coordinates in the rotating coordinate system at any x-ray gantry angle other than the reference position are designated as (X', Y', Z') which relates to (X, Y, Z) according to

$$\begin{bmatrix} X \\ Y \\ Z \end{bmatrix} = [\mathbf{R}(\theta)] \begin{bmatrix} X' \\ Y' \\ Z' \end{bmatrix}. \tag{1}$$

The rotation matrix, $\mathbf{R}(\theta)$, is defined as

$$\mathbf{R}(\theta) = \begin{bmatrix} \cos(\theta) & 0 & \sin(\theta) \\ 0 & 1 & 0 \\ -\sin(\theta) & 0 & \cos(\theta) \end{bmatrix} \tag{2}$$

where θ is the x-ray gantry angle relative to the reference coordinate system.

The relationship between the reference patient space (X, Y, Z) and its projection onto the detector domain, (U, V), is given by

$$U = \frac{FX}{S+Z} \tag{3}$$

$$V = \frac{FY}{S+Z} \tag{4}$$

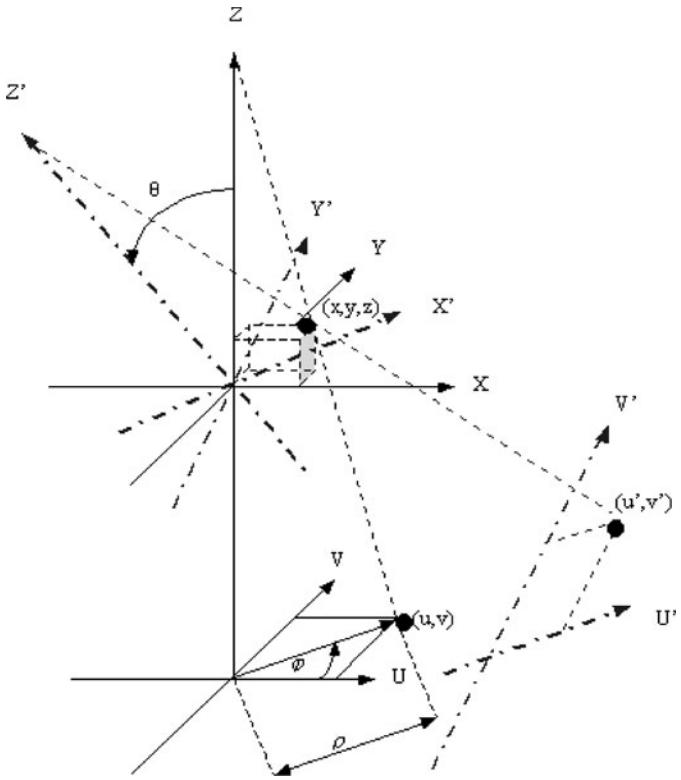

Figure 1. Definition of coordinate system. The x-ray source, located at Z, rotates about the Y-axis through angle θ. (X, Y, Z) is the reference and (X', Y', Z') is the rotated 3D coordinate system. Corresponding projection domains are designated as (U, V) and $(U'V')$, respectively. The black dots indicate the location of the seed in 3D and projected coordinate systems.

where F is the distance between the x-ray source and the detector, and S is the distance between the source and the axis of rotation.

2.2. Hough transform

The Hough transform developed by Paul Hough in 1962 (Hough) has become a standard tool in image processing and computer vision for detection of lines, circles and ellipses. Generalized Hough transform can detect arbitrary shapes, given a parametrized description of the shape in question. For the task at hand the concept of Hough transform is used to describe the path of a given seed as it is projected onto the detector plane at different gantry angles (figure 2). First, we express the projection of a 3D point onto the detector space in polar coordinates (ρ, φ):

$$\rho = (U^2 + V^2)^{1/2} \tag{5}$$

$$\varphi = \tan^{-1}(V/U). \tag{6}$$

Remembering the relationships established in equations (1)–(4), a set of 3D seed coordinates (X, Y, Z) (dropping the prime sign) at a gantry angle θ is transformed into a 2D point (ρ, φ) by

$$\rho = \frac{F[(X\cos(\theta) + Z\sin(\theta))^2 + Y^2]^{1/2}}{S - X\sin(\theta) + Z\cos(\theta)} \tag{7}$$

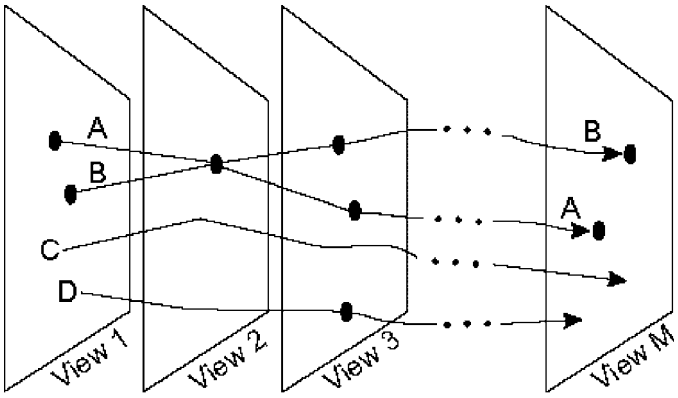

Figure 2. The Hough trajectory of a given seed is unique as depicted by path A. Black circles indicate the x-ray projection of the seed centroids. The paths intersect when seeds are ambiguously identified due to superposition. For example, paths A and B meet at view 2 where two seed images completely overlap. Hough trajectory C does not match with any seed, thus will be discarded. Trajectory D has only one 'hit' at view 3 most likely due to false positive identification. This path will accumulate a low score and will be eliminated.

$$\varphi = \tan^{-1}\left(\frac{Y}{X\cos(\theta) + Z\sin(\theta)}\right). \tag{8}$$

The Hough transform equations in (7) and (8) are functions of gantry angle and thus describe the trajectory of a given set of 3D seed coordinates as projected onto the 2D detector domain. For each seed this path is unique. Or, conversely stated, given a Hough trajectory the 3D seed coordinates can be determined.

2.3. 3D seed reconstruction

The task of seed reconstruction begins by defining the 3D search space, which encompasses the entire volume of the seed implant. One strategy is to determine a smallest rectangle that encloses all the seeds appearing on the recorded projection data. This is performed on a few representative views, e.g. two extreme projection angles and another at half way. When backprojected onto the x-ray source, the intersection of the pyramids defined by the bounding rectangles (base) and the source (apex) will form a volume which contains all the implanted seeds. This volume represents the 3D search space. In order to facilitate the numerical implementation the volume is quantized into cubic voxels at a resolution that matches the pixel size of the x-ray data corrected for magnification.

Each voxel in the search volume described above is a potential seed location. Then the objective is to find a voxel whose Hough-transformed path coincides with a seed in each of the recorded views. To accomplish this, first Hough trajectory is calculated using equations (7) and (8). Then for each view the distance between the path and the nearest seed is examined. The Hough path is extended to the next view if the distance is within a certain range, e.g. one seed length, otherwise the trajectory is terminated. Through this process the majority of the seed candidates is eliminated from the 3D search volume. Next, the Hough trajectories of the survived candidates are scored. For each view the distances between a given seed and the paths that are associated with the seed are compared. The path that is closest to the seed being examined receives a score of one and the rest zero. In the event that two or more paths share the closest distance within a small range, e.g. two detector pixels, these paths are

(a)

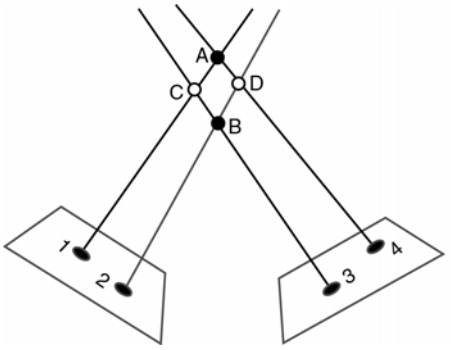

	Hough path	Score
True seeds	A: 1→4	2
	B: 2→3	2
False seeds	C: 1→3	2
	D: 2→4	2

(b)

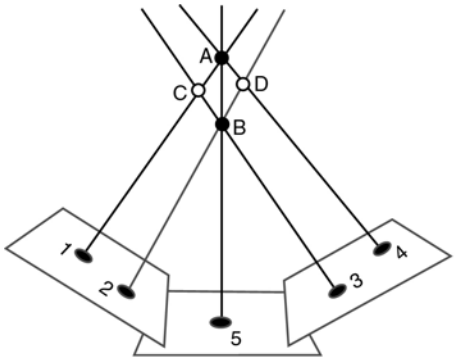

	Hough path	Score
True seeds	A: 1→4→5	3
	B: 2→3→5	3
False seeds	C: 1→3	2
	D: 2→4	2

Figure 3. (a) If there is an insufficient number of views available, ambiguous seed identification could result. (b) The classic case of ambiguous seed identity shown in (a) can be resolved by adding a projection as shown here.

considered to represent overlapping seeds and will each receive a score of one. Finally, the score is accumulated along each path from different views and the top N candidates (where N is the maximum possible number of seeds) are selected as being associated with the 3D seed positions.

Given a set of projection data acquired over M views, the top N candidates should have a score of M. However, if there is an insufficient number of views available, ambiguous seed identification can result as illustrated in figure 3(a). In this example, there are two seeds (A and B) imaged at two gantry angles. The projection of these seeds will appear as points 1, 2, 3 and 4, on the detector plane. Accordingly, the Hough transform method will generate four unique paths as shown in the table. However, all of these paths will accumulate the same number of 'hit' points. Consequently, even the candidates C and D will be classified erroneously as seeds. This classic case of ambiguous seed identity can be resolved by adding an extra (the third) view as shown in figure 3(b).

Figure 4 illustrates the ability of the proposed method to reconstruct seeds even when none of the views has identified all of the seeds. In this example, three seeds (A, B and C) are imaged at three different angles. Each view records only two out of three seeds due to superposition. In the search space there exist other seed candidates D, E and F, whose projections will coincide with those of the true seeds. But the Hough trajectory scores can

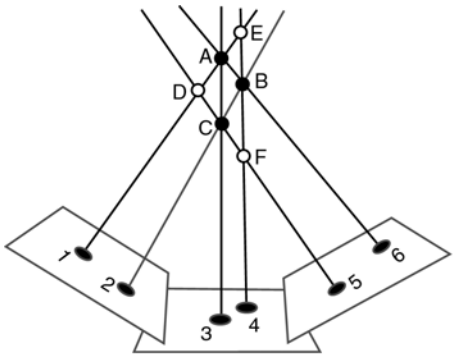

	Hough path	Score
True seeds	A: 1 → 3 → 6	3
	B: 2 → 4 → 6	3
	C: 2 → 3 → 5	3
False seeds	D: 1 → 5	2
	E: 1 → 4	2
	F: 4 → 5	2

Figure 4. Illustration of how the Hough trajectory method can reconstruct seeds even when none of the views has identified all of the seeds.

help differentiate the true seeds from the false positives. The true seeds A, B and C will receive a score of three while the other candidates will have only two 'hit' points. Selection of top N ($N = 3$) candidates will correctly reconstruct seeds A, B and C in 3D space.

Under ideal conditions with infinite detector resolution and perfect geometry, the algorithm outlined above will yield accurate results using just a few projections, e.g. three or four. In practice, however, noise in the data arising from uncertainties associated with the seed segmentation process and patient movement may not permit the Hough trajectory of a true seed candidate to accumulate the possible score of M since another path may end up passing closer to a seed of interest in a certain view. For this reason, it is advantageous to use a greater number of views when constructing the Hough trajectories.

3. Results

Both simulation and empirical data were used to verify the algorithm. The algorithm was prototyped in Matlab, coded in C++, and tested on a PC with a 2 GHz Pentium IV processor.

3.1. Simulated data

For simulation studies, 125 seeds were generated in $5 \times 5 \times 5$ cubic formation at 1 cm intervals. Subsequently, the second and the fourth layers were shifted by 0.5 cm in the Y-direction while the third and the fifth layers were offset in the X-direction by the same amount. These offsets were introduced in order to generate data that contained superposed seeds when projected at different gantry angles. The centre of the seed distribution was located at the isocentre at a distance of 100 cm from the x-ray source. The centroids of the seeds were projected onto the detector planes located at 140 cm from the x-ray source. The pixel resolution of the detector was 0.032 cm, which is equivalent to that of our 6 inch fluoroscopy unit. The projection data were generated in 1° increments at gantry angles ranging from 160 to 200° with the 180° orientation being the anterior–posterior direction. About half of the projections contained completely superposed seeds. The number of unidentified seeds due to superposition ranged from 3 to 24. Figure 5 shows some of the projection data. Hough trajectories were generated for each voxel within the implant volume as described in section 2.3. The voxel size, 0.023 cm, is the detector resolution demagnified by the ratio of source-to-detector and source-to-prostate distances to account for beam divergence.

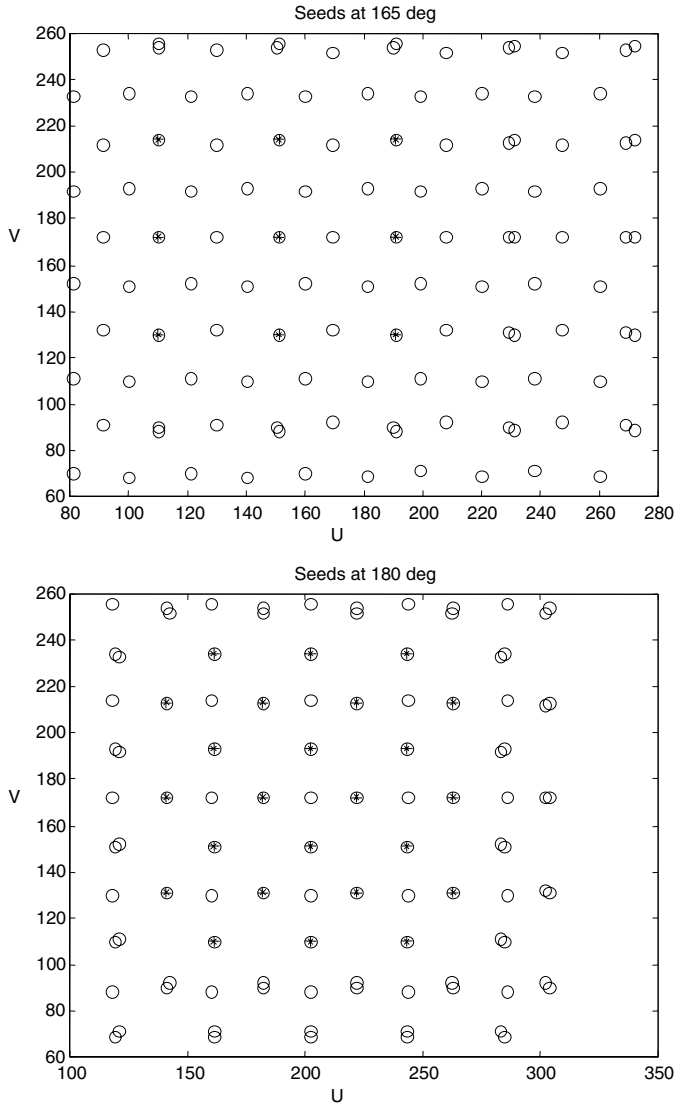

Figure 5. Examples of projection data used in the simulation study. Spatial units are in pixels. Centre of circles indicates the seed centroid location. Completely superposed seeds are marked by an asterisk. 116 out of 125 seeds are identifiable in the 165° projection (top) whereas only 101 seeds are identified in the 180° projection (bottom).

3.1.1. Reconstruction from complete dataset. In the first simulation study, it was assumed that a complete dataset was available and none of the views used in reconstruction had missing seeds. The input data were preferentially selected so that only the projections containing all 125 seeds were used. The number of projections used to reconstruct the seeds was varied from three to nine. Table 1 tabulates the results of seed reconstruction. The errors in seed locations relative to the truth were less than 0.013, 0.019 and 0.045 cm in the *X, Y* and *Z* directions when using four or more projections.

Table 1. Results of 3D seed reconstruction from complete datasets. The number of views used ranged from three to nine. All projections contained the possible number of seeds of 125.

Views (projection angle)	Number of views used						
	3	4	5	6	7	8	9
161	✓	✓	✓	✓	✓	✓	✓
163				✓	✓	✓	✓
171		✓	✓	✓	✓	✓	✓
176					✓	✓	✓
184	✓	✓	✓	✓	✓	✓	✓
186						✓	✓
191			✓	✓	✓	✓	✓
197							✓
200	✓	✓	✓	✓	✓	✓	✓
Max *X* error (cm)	4.12	0.013	0.013	0.013	0.013	0.013	0.013
Max *Y* error (cm)	4.50	0.019	0.019	0.015	0.015	0.015	0.015
Max *Z* error (cm)	1.55	0.045	0.029	0.029	0.029	0.029	0.029

Table 2. Results of 3D seed reconstruction from incomplete datasets: easy cases. Only those views with missing seeds were used. The number of views used in reconstruction was incrementally reduced by removing the views with the least number of identified seeds. Therefore, these trials represent relatively easy cases. The possible number of seeds was 125.

Views (projection angle)	Number of seeds identified	Number of views used						
		14	13	12	11	10	9	8
164	122	✓	✓	✓	✓	✓	✓	✓
165	116	✓	✓	✓	✓	✓	✓	✓
166	114	✓	✓	✓	✓			
167	114	✓	✓	✓	✓	✓	✓	
168	120	✓	✓	✓	✓	✓	✓	✓
178	118	✓	✓	✓	✓	✓	✓	✓
179	108	✓	✓	✓				
180	101	✓						
181	105	✓	✓					
182	115	✓	✓	✓	✓	✓	✓	✓
193	117	✓	✓	✓	✓	✓	✓	✓
194	114	✓	✓	✓	✓	✓		
195	116	✓	✓	✓	✓	✓	✓	✓
196	122	✓	✓	✓	✓	✓	✓	✓
Max *X* error (cm)	–	0.011	0.011	0.013	0.011	0.011	0.011	1.01
Max *Y* error (cm)	–	0.013	0.015	0.015	0.015	0.015	0.015	1.01
Max *Z* error (cm)	–	0.047	0.043	0.043	0.043	0.047	0.055	0.55

3.1.2. Reconstruction from incomplete dataset. In order to test the ability of the Hough method to reconstruct the seeds from a set of incomplete data, only those projections with 'missing' (superposed) seeds were selected. Table 2 lists 14 such projections. The number of identified seeds ranged from 101 to 122 out of 125 total. Utilizing all 14 projections the Hough trajectory method computed the 3D seed coordinates with excellent accuracy. The maximum errors in the *X*, *Y* and *Z* directions were 0.011, 0.013 and 0.047 cm, respectively.

Table 3. Results of 3D seed reconstruction from incomplete datasets: difficult cases. Only those views with missing seeds were used. The number of views used in reconstruction was incrementally reduced by removing the views with the highest number of identified seeds. Therefore, these trials represent challenging cases. The possible number of seeds was 125.

Views (projection angle)	Number of seeds identified	Number of views used			
		14	13	12	11
164	122	✓			
165	116	✓	✓	✓	✓
166	114	✓	✓	✓	✓
167	114	✓	✓	✓	✓
168	120	✓	✓	✓	
178	118	✓	✓	✓	✓
179	108	✓	✓	✓	✓
180	101	✓	✓	✓	✓
181	105	✓	✓	✓	✓
182	115	✓	✓	✓	✓
193	117	✓	✓	✓	✓
194	114	✓	✓	✓	✓
195	116	✓	✓	✓	✓
196	122	✓	✓		
Max *X* error (cm)	–	0.011	0.011	0.011	0.49
Max *Y* error (cm)	–	0.013	0.013	0.013	0.49
Max *Z* error (cm)	–	0.047	0.056	0.063	0.48

The exercise successfully demonstrates that the feature space trajectory can accurately reconstruct 3D seed positions even when none of the views have identified all the seeds. But it was not clear as to how much data are sufficient for faithful reconstruction. In order to answer the question the number of projections was reduced progressively until localization errors became unacceptable. Projections were removed from the input dataset starting with the one having the least number of identified seeds (i.e., projection angle 180° with 101 seeds) and the next (i.e., projection angle 181° with 105 seeds) and so on. The results shown in table 2 indicate that as few as nine views can successfully reconstruct all 125 seeds. The number of available seeds for the nine views ranged from 114 to 122.

We have also simulated very difficult cases in which the views that contain a large number of identified seeds (useful information) were excluded. Views were removed from the input dataset starting with the one having the highest number of identified seeds (i.e., projection angle 164 with 122 seeds). The results tabulated in table 3 indicate that at least 12 projections are needed when the dataset is highly incomplete with a large number of missing seeds. The number of available seeds for the 12 views ranged from 101 to 120.

3.2. Phantom study

A physical phantom study was conducted in order to evaluate the algorithm in a clinically relevant setting. A prostate phantom was implanted with 61 dummy I-125 seeds and projection data were obtained with a radiotherapy simulator (SLS-14, Elekta Oncology Systems, Crawley, UK) using the 6 inch image intensifier mode over a 40° angular span. The radiotherapy simulator is used routinely for prostate brachytherapy procedures in our clinic. Nine views were captured at 5° increments from 160° to 200° with a frame grabber (Meteor-II, Matrox Graphics, Dorval, Canada) into a PC. The gantry angle of 180° indicates the anterior–posterior

Table 4. Number of seeds identified by the automated seed detection algorithm for the phantom experiment. The views with asterisks were not used in seed reconstruction.

Views (projection angle)	Number of seeds identified
160	59
165*	61
170	61
175	60
180*	61
185	59
190	59
195	60
200*	61

orientation. The seed centroids on each view were then automatically determined. The process begins with the correction for geometric distortion introduced by the image intensifier (Cho *et al* 1995). Next, the seeds are automatically segmented through a series of image processing operations (Cho 2000). First, a grayscale morphological top hat operation is applied in order to separate the seeds from the background. This is followed by an automated grayscale thresholding step using a discriminant analysis. Finally, the resultant, binary seed images are examined through template matching to locate the seed centroids. The results of automated seed segmentation were compared with the manually determined seed centroids. Agreements were within two pixels (or 0.064 cm). There were a few superposed seeds that were not identified by the seed detection algorithm. However, no manual interventions were made to identify the missing seeds. Therefore, the superposed seeds remained classified as single seeds. Table 4 shows the number of seeds that were automatically identified for each view. Using all nine views the Hough trajectory algorithm successfully reconstructed all 61 seeds. To explore the limit of the algorithm the number of views used was reduced until reconstruction errors began to exceed 0.05 cm or 10% of the seed length. This limit was reached when more than three views, which contributed the most to reconstruction (i.e., views with the highest number of seeds), were removed. The three views that were excluded from the input contained all 61 seeds and are identified by asterisks in table 4. In order to qualitatively evaluate the accuracy of reconstruction using the reduced number of views (six instead of nine) the 3D solutions were projected onto views 165°, 180° and 200°, as shown in figure 6. Visual inspection of the figure reveals that the large majority of the centroid projections fall within the seed images. Only a small fraction of the projected centroids is off by a few pixels. These errors are due to uncertainties introduced in the seed segmentation and detection steps.

For quantitative assessment the results were compared with those from a back projection based reconstruction. A previously reported fast cross-projection method was used to calculate the 3D seed coordinates using the views 165°, 180° and 200°. The overall accuracy of the fast cross-projection algorithm including the distortion correction, seed detection and reconstruction has been previously reported as 0.041, 0.041 and 0.022 cm in the X, Y and Z directions, respectively (Narayanan *et al* 2002). The results of the Hough trajectory method differed only slightly from those of the cross-projection technique. The RMS errors and standard deviations of the Hough method relative to the cross-projection method were 0.0035 ± 0.0042 cm, 0.0039 ± 0.0045 cm and 0.012 ± 0.015 cm in the X, Y and Z directions, respectively. The maximum errors were 0.0093, 0.011 and 0.038 cm.

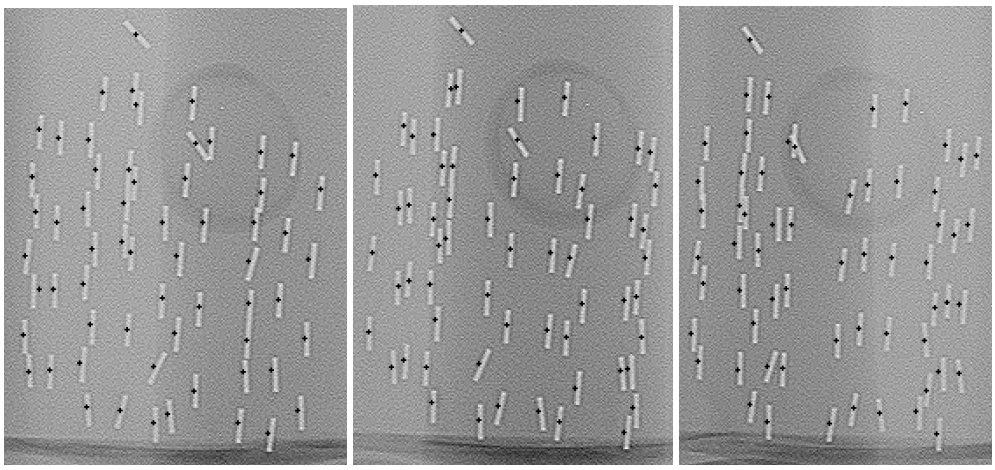

Figure 6. For qualitative evaluation of reconstruction accuracy the 3D solutions (seed centroids) were projected onto fluoroscopy images. From left to right, there are projections for 165°, 180° and 200°. Since these views have no superposed seeds and have wide angular span, they are suited for verification of reconstruction via re-projection. All 61 seeds are verified. The black crosses mark the re-projected centroids.

4. Discussion

The Hough trajectory method takes a significantly different approach from the previously developed algorithms. Instead of back projection, the present technique works in the forward direction. It begins in the 3D seed space and seeks to find a Hough trajectory in the projection domain that is unique to a given seed. The main advantage of the present algorithm is its ability to localize 100% of the implanted seeds from an incomplete dataset. For example, in commonly used three-view back projection methods, given $N - p$, $N - q$ and $N - r$ seeds in each of three views (where N is the total number of implanted seeds and $p > q > r$) the maximum number of seeds that can be reconstructed is only $N - p$. In comparison, the Hough method can reconstruct all N seeds.

For faithful reconstruction the proposed method requires a moderate number of views. The required number of views depends on the extent of unidentifiable seeds on each projection. For a small amount of missing seeds (of the order of 4%) as few as 6 views are sufficient while for a more difficult case (e.g., up to 20% missing) 12 or more views may be needed. In clinical practice, however, the number of missing seeds in a given view rarely exceeds 10% of the total. Therefore, it is estimated that 6 to 9 views should be sufficient for most cases. However, in the presence of significant noise due to imperfections such as uncorrected gantry wobble or patient motion a larger number of views will be required.

It may be argued that back projection methods can also be used for faithful reconstruction if many views are provided from which to select three views containing all N seeds. However, this approach may not be robust as there is no guarantee that all N seeds will be identified in at least three views among the acquired projections. One obstacle is the problem of false positives. That is, even when N objects have been detected in a view, they may consist of $N - p$ seeds and p false seeds. False positives do occur in automated processes as high contrast objects such as thresholded fragments of bones and catheter wires mimic the seeds. Furthermore, when seeds are heavily clustered, it is possible that more than the actual number of seeds is detected in one cluster while a fewer number in another cluster thus erroneously

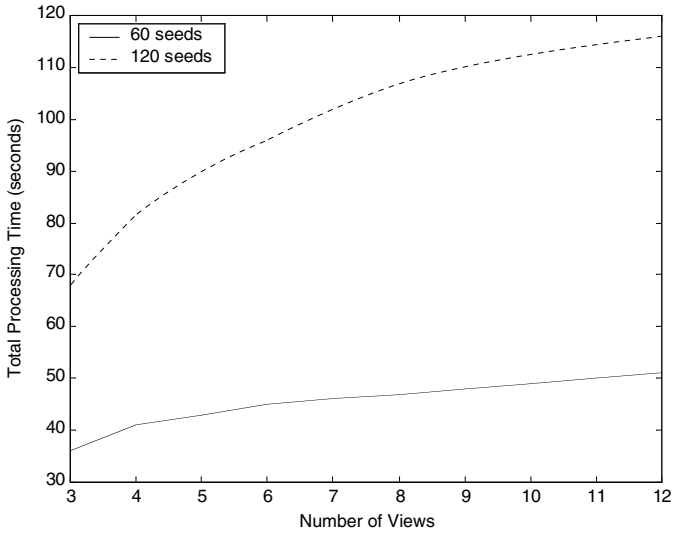

Figure 7. Processing time as a function of number of views and seeds.

giving a total of N seeds. Therefore, obtaining three views with correctly identified N seeds is not necessarily an easy task.

The computation times as a function of number of views and seeds are plotted in figure 7. Since a large majority of the seed candidates and associated Hough trajectories are terminated quickly (see section 2.3) the overhead to process additional views diminishes as the number of views increases. For example, in the 60-seed case, as the number of views is tripled from three to nine, the calculation time increases only by 33% compared to the 25% increase when the number of views is doubled. Relative to the number of seeds, the computation time increases almost linearly. For 120 seeds and nine views, the processing time was 110 s on a 2 MHz PC. Calculation time can be shortened by parallelizing the algorithm so that multiple Hough trajectories can be processed simultaneously.

5. Conclusion

The proposed method based on the Hough transform can determine the 3D position of brachytherapy seeds even when some of the seeds are undetected in x-ray projections due to superposition. The method also has the ability to incorporate a large number of views without incurring major computing cost. As such, the technique has the potential for clinical application.

Acknowledgments

This work was supported in part by grants from the National Institutes of Health R21-CA89061 and the Department of Defense DAMD17-03-1-0033.

References

Altschuler M D, Findlay P A and Epperson R D 1983 Rapid, accurate, three-dimensional location of multiple seeds in implant radiotherapy treatment planning *Phys. Med. Biol.* **28** 1305–18

Amols H I and Rosen I I 1981 A three-film technique for reconstruction radioactive seed implants *Med. Phys.* **8** 210–4

Biggs P J and Kelley D M 1983 Geometric reconstruction of seed implants using a three-film technique *Med. Phys.* **10** 701–4

Cho P S 2000 Computerized segmentation of clustered seeds in prostate brachytherapy *Proc. 13th Int. Conf. on Computers in Radiotherapy* ed W Schlegel and T Bortfeld (Heidelberg: Springer) pp 105–7

Cho P S, Johnson R H and Griffin T W 1995 Cone-beam CT for radiotherapy applications *Phys. Med. Biol.* **40** 1863–83

Hough P V C 1962 A method and means for recognizing complex patterns US Patent 3,069,654

Lam S T, Marks R J II and Cho P S 2002 Three dimensional seed reconstruction in prostate brachytherapy using Hough transformations *Proc. SPIE* **4790** 443–53

Nag S, Bice W and deWyngaert K *et al* 2000 The American Brachytherapy Society recommendations for permanent prostate brachyherapy post-implant dosimetric analysis *Int. J. Radiat. Oncol. Biol. Phys.* **46** 221–30

Narayanan S, Cho P S and Marks R J II 2002 Fast cross-projection algorithm for reconstruction of seeds in prostate brachytherapy *Med. Phys.* **29** 1572–9

Rosenthal M S and Nath R 1983 An automatic seed identification technique for interstitial implants using three isocentric radiographs *Med. Phys.* **10** 475–9

Siddon R L and Chin L M 1985 Two-film brachytherapy reconstruction algorithm *Med. Phys.* **12** 77–83

Todor D A, Cohen G N, Amols H I and Zaider M 2002 Operator-free, film-based 3D seed reconstruction in brachytherapy *Phys. Med. Biol.* **47** 2031–48

Tubic D, Zaccarin A, Beaulieu L and Pouliot J 2001 Automated seed detection and three-dimensional reconstruction: II. Reconstruction of permanent implants using simulated annealing *Med. Phys.* **28** 2272–9